Characterization and biofouling potential analysis of two cyanobacterial strains isolated from Cape Verde and Morocco

Maria J. Romeu[a,b †], João Morais[c,d †], Luciana C. Gomes[a,b], Raquel Silva[c], Vítor Vasconcelos[c,d*], Filipe J. M. Mergulhão[a,b*]

[a]LEPABE - Laboratory for Process Engineering, Environment, Biotechnology and Energy, Faculty of Engineering, University of Porto, Rua Dr. Roberto Frias, 4200-465 Porto, Portugal
[b]ALiCE - Associate Laboratory in Chemical Engineering, Faculty of Engineering, University of Porto, Rua Dr. Roberto Frias, 4200-465 Porto, Portugal
[c]CIIMAR – Interdisciplinary Centre of Marine and Environmental Research, University of Porto, Terminal de Cruzeiros do Porto de Leixões, Av. General Norton de Matos s/n, 4450-208 Matosinhos, Portugal
[d]Department of Biology, Faculty of Sciences, University of Porto, Rua do Campo Alegre, 4169-007, Porto, Portugal

† These authors contributed equally to this work.

*** Corresponding authors:**
Vítor Vasconcelos
Department of Biology
Faculty of Sciences, University of Porto
Rua do Campo Alegre, 4169-007, Porto, Portugal
Phone: (+351) 223401800
Fax: (+351) 223390608
Email: vmvascon@fc.up.pt

Filipe J. M. Mergulhão
Chemical Engineering Department
Faculty of Engineering, University of Porto
Rua Dr. Roberto Frias 4200-465, Porto, Portugal
Phone: (+351) 225081668
Fax: (+351) 5081449
Email: filipem@fe.up.pt

ABSTRACT

Cyanobacteria are new sources of value-added compounds but also ubiquitous and harmful microfoulers on marine biofouling. In this work, the isolation and identification of two cyanobacterial strains isolated from Cape Verde and Morocco, as well as their biofilm-forming ability on glass and Perspex under controlled hydrodynamic conditions were performed. Phylogenetic analysis revealed that cyanobacterial strains isolated belong to *Leptothoe* and *Jaaginema* clade (*Leptothoe* sp. LEGE 181153 and *Jaaginema* sp. LEGE 191154). From quantitative and qualitative data of wet weight, chlorophyll *a* content and biofilm thickness obtained by Optical Coherence Tomography (OCT), no significant differences were found in biofilms developed by the same cyanobacterial strain on different surfaces (glass and Perspex). However, the biofilm-forming potential of *Leptothoe* sp. LEGE 181153 proved to be higher when compared to *Jaaginema* sp. LEGE 191154, particularly at the maturation stage of biofilm development. Three-dimensional biofilm images obtained from Confocal Laser Scanning Microscopy (CLSM) showed different patterns between both cyanobacterial strains and also among the two surfaces. Since standard methodologies to evaluate cyanobacterial biofilms formation, as well as two different optical imaging techniques were used, this work also highlights the possibility to integrate different techniques to evaluate a complex phenomenon like cyanobacterial biofilm development.

Keywords: filamentous cyanobacteria**,** cyanobacteria isolation, cyanobacteria characterization, marine biofouling, cyanobacterial biofilms, surface effect

INTRODUCTION

Cyanobacteria are a widespread and significant group of photosynthetic prokaryotes responsible for the accumulation of oxygen in the Earth's environment (Lyons, Reinhard and Planavsky 2014) and the evolution of eukaryotic organisms, according to the widely accepted endosymbiotic theory (Ku *et al.* 2015). They contribute to the nitrogen and carbon biogeochemical cycles, and can persist in harsh conditions due to their high adaptability (Berg and Sutula 2015; Anderson 2016). The metabolic flexibility between oxygen photosynthesis and respiration (Vermaas 2001; Mullineaux 2014) allows them to thrive in diverse environments. While some cyanobacteria can be associated with heterotrophic organisms in the desert to facilitate the productivity of soil crust (Pointing and Belnap 2012), some of them are the primary colonizers of ice sheets (Vincent 2000). Therefore, these particular bacteria are common in many habitats such as lakes, ponds, springs, wetlands, streams, rivers, soil crust, microbial mats, sands, and rocks (Ramos *et al.* 2018). Cyanobacteria strains present a considerable morphological diversity, comprising distinct degrees of complexity (Schirrmeister, Antonelli and Bagheri 2011). When compared with unicellular coccoid morphology, filamentous phenotype can be beneficial since it has a higher resistance to stress and predation, as well as improved resource acquisition (Claessen *et al.* 2014).

Cyanobacteria have been considered promising organisms for biotechnological processes due to the broad spectrum of secondary metabolites produced by some strains (Lau, Matsui and Abdullah 2015; Manirafasha *et al.* 2016). These added-value compounds can be applied to enhance the sustainable production of food and green energy sources (Singh *et al.* 2017), and they can also be used for medical purposes due to their antioxidant, anticancer, and anti-inflammatory properties (Pagels *et al.* 2019). However, cyanobacteria can also have a

detrimental impact on human purposes due to their ability to produce toxins (Breinlinger *et al.* 2021), promote cyanobacterial blooms (Huisman *et al.* 2018), and participate in the biofouling processes (Carvalho 2018). Marine biofouling consequences include environmental, economic, ecological, and health concerns (Caruso 2020). The corrosion of different facilities and equipment may lead to incorrect measurements of submerged sensors and measuring devices, and high costs related to cleaning and/or repainting (Delauney, Compare and Lehaitre 2010), contributing to the industrial and economic consequences associated with biofouling. Moreover, the introduction and spread of invasive non-indigenous pathogens on marine vessels between different ecosystems (Davidson *et al.* 2009; Georgiades *et al.* 2021) and the contamination of aquaculture facilities (Bannister *et al.* 2019) may impact the ecology and global health. In the environmental field, marine biofouling can lead to increased fuel consumption by ships and consequently, enhanced air pollution and greenhouse gas emissions (Hunsucker *et al.* 2018).

Marine biofouling is a complex process and it has been suggested that the adhesion and biofilm development by microfouler organisms may affect the continuous biofouling process, particularly for larval recruitment and settlement of macrofouler organisms (Antunes, Leão and Vasconcelos 2019; Dobretsov and Rittschof 2020). Although their prevalence depends on the surface, geographical area and environmental settings, cyanobacteria are microfoulers and the major constituents of marine biofilms together with diatoms (Bharti, Velmourougane and Prasanna 2017; Antunes *et al.* 2020; Papadatou *et al.* 2021).These organisms produce extracellular polymeric substances (EPS), which are essential compounds of biofilm communities for maintaining their cohesion, structure, and stability (Limoli, Jones and Wozniak 2015; Rossi and De Philippis 2015; Anderson 2016).

Marine biofilms are affected by several factors, including physical, chemical, and biological drivers (Caruso 2020; Faria *et al.* 2020b, 2021b). After the formation of the conditioning film

comprising the adsorption of molecules (proteins, carbohydrates, etc.) from the surrounding environment, the second step in the biofouling process involves cell adhesion. Surface binding is considered a critical survival mechanism for enhancing organism interactions and accessing nutritional resources (Dang and Lovell 2016). Different materials are used in marine submerged man-made equipment, like aquaculture facilities (King *et al.* 2006; Cai and Arias 2017), underwater windows, sensors and measuring devices (Roy 1994; Taylor 1996; Davies and Rajapakse 2013), protective equipment, swim platforms, ship and boat structures, and anchors (Taylor 1996; Mansour and Liu 2008; Molland 2008; Davies and Rajapakse 2013), which are susceptible to biofouling. Therefore, studies focused on the effects of substrate properties and organisms' variability in the growth stages of biofilms, and their composition, structure and behaviour are of great importance (Faria et al., 2021a, 2021c; Faria et al., 2020a). Indeed, previous studies showed a broad diversity in the protein expression profiles of cyanobacterial biofilms isolated from different sites (Romeu *et al.* 2020), which may be a result of the adaptation of these organisms to the specific environmental niche that they occupy, such as their site of isolation and the nutritional availability at that site (Bragg, Thomas and Baudouin-Cornu 2006; Lv, Li and Niu 2008). Through the simultaneous analysis of physiological characteristics, the distribution in the environment, and the genome and/or proteomic profiles, it is possible to identify the environmental factors that are most important to drive evolution and shape populations. For instance, greater depths are associated with lower light intensity and temperature, but also with higher content of phosphorus (Coleman and Chisholm 2007). For instance, to cyanobacterium *Prochlorococcus*, phosphorus availability is a key ecological factor and a potential driver of evolution (Lv, Li and Niu 2008). Different *Prochlorococcus* strains possess distinct physiological adaptations for dealing with the low phosphorus availability, including the replacement of phospholipids with sulfolipids (Van Mooy *et al.* 2006), growth

in a more limited range of phosphorus sources (Moore *et al.* 2005), and the upregulation of known phosphorus-assimilation genes and novel genes, which may enable them to tolerate phosphorus starvation periods (Martiny, Coleman and Chisholm 2006). Moreover, recent metagenomic studies showed that the abundance of phosphate transport genes is also correlated with phosphorus availability (Rusch *et al.* 2007). In the low-phosphorus waters of the Caribbean, the gene encoding a phosphate-binding protein is more abundant compared with the higher-phosphorus waters of the Pacific.

The main novelty of this study is the isolation, identification (morphological characterization), and assessment of the biofilm-formation potential of cyanobacterial strains isolated from underexplored marine environments and locations across the coast of Cape Verde and Morocco. These are locations with unknown biodiversity that will provide new knowledge and tools to understand the impact of global changes in temperate areas. Cyanobacterial strains from these genera seem to be quite frequent at least in the Atlantic Ocean, North Aegean Sea, and Mediterranean Sea (Foster *et al.* 2009; Konstantinou *et al.* 2018, 2019; Ramos *et al.* 2018). Since they are distributed around dissimilar geographies, including different continents and port areas, this cosmopolitan distribution highlights the importance of studying biofilm formation by these organisms, which in turn, presents a significant concern in the public health, environment, and aquatic ecology. Given the relevance of cyanobacteria on marine biofouling, their biofilm-forming ability was assessed for the first time in a long-term assay under controlled hydrodynamic conditions, which mimics marine environments (Romeu *et al.* 2019), and using two different surfaces as the substratum for biofilm formation (glass and Perspex). These materials represent submerged artificial surfaces typically found on different aquatic apparatus such as sensors, flotation spheres, moored buoys, underwater cameras, aquaculture equipment, measuring devices, or even in underwater windows of boats (Taylor 1996; Blain *et al.* 2004; King *et al.* 2006) that

can be affected by biofouling. Additionally, given the broad spectrum of promising secondary metabolites and value-added compounds produced by cyanobacteria (Lau, Matsui and Abdullah 2015) that can be used in biotechnological applications, cosmetics, feed, and food industries (Manirafasha *et al.* 2016), and medical purposes (Pagels *et al.* 2019), this kind of study can also be useful in different research fields.

MATERIALS AND METHODS

Sampling and Isolation

Environmental samples were collected on July 11, 2019, near Mrizika Beach, Morroco (32°57'31.3"N 8°46'34.1"W) from a dried soil crust and on April 24, 2019, at Calhau, Cape Verde (São Vicente Island - 16°51'07.6"N 24°51'58.8"W) scraping from a port boat ramp with the help of a previously cleaned knife (Figure 1). Samples were transferred to 15 ml tubes with Z8 medium (Kotai 1972) supplemented with 25 $g.l^{-1}$ of synthetic sea salts (Tropic Marin) and B_{12} vitamin (Sigma Aldrich, Merck, Saint Louis, MO, USA) (Croft, Warren and Smith 2006; Helliwell *et al.* 2016) until further analysis. Isolation of cyanobacterial isolates was performed using the streak plate method (Rippka 1988). Briefly, using a sterile plastic Pasteur pipette, a homogeneous drop from each environmental sample was inoculated in different agar plates with Z8 medium, and with a loop, each sample was spread, making successive smears in the different quadrants of the plate. After approximately 1 month of growth under 14 h light (10–30 μmol photons m^{-2} s^{-1})/10 h dark cycles, at 25 °C, isolated cells or filaments were picked up using a sterile surgical blade and transferred to 50 ml culture flasks with a liquid medium, growing in the previously described conditions. After 2-3 weeks of growth, isolation was confirmed by checking samples under the microscope.

DNA Extraction, 16S rRNA Gene Amplification (PCR), and Sequencing

The two filamentous cyanobacterial isolates obtained in this work were grown in 50 ml flasks in the conditions previously described and harvested by centrifugation (5,000 *g* for 5 min at 4° C) after 2-3 weeks. Total genomic DNA was extracted using the commercial PureLink Genomic DNA Mini Kit (Invitrogen, USA), according to the manufacturer's instructions provided for Gram-negative bacteria. To obtain the 16S rRNA gene sequence, PCR amplification was performed using the oligonucleotide primers set 27F and 23S30R (Table 1). PCR reactions were performed in a final volume of 20 µl containing 1× Green GoTaq Flexi Buffer, 2.5 mM of $MgCl_2$, 125.0 mM of each deoxynucleotide triphosphate, 1.0 µM of each primer, 0.5 U of GoTaq Flexi DNA Polymerase (Promega, Madison, WI, USA), 10 $mg.ml^{-1}$ of bovine serum albumin (BSA), and 10–30 ng of template DNA, on a Veriti™ 96-Well Thermal Cycler (Applied Biosystems™, USA). The PCR conditions were as follows: initial denaturation at 94 °C for 5 min, followed by 10 cycles of denaturation at 94 °C for 45 s, annealing at 57 °C for 45 s, and extension at 72 °C for 2 min, followed by 25 cycles of denaturation at 92 °C for 45 s, annealing at 54 °C for 45 s, and extension at 72 °C for 2 min with a final elongation step at 72 °C for 7 min. The PCR reactions were performed in duplicate. PCR products were separated by 1.5% agarose gel stained with SYBR® safe (Invitrogen, Waltham, MA, USA), and DNA fragments with the expected size were excised and purified using NZYGelpure (NzyTech, Genes and Enzymes, Lisbon, Portugal) according to the manufacturer's instructions. Since the sequences were obtained by direct sequencing of purified amplicons, CYA359F, CYA781R, and 1494R internal primers (Table 1) were used to improve the quality of the sequences. Sequencing was performed at GATC Biotech (Ebersberg, Germany) and the nucleotide sequences obtained were manually inspected for quality and assembled using the Geneious 11.1.5 software (Biomatters Ltd., Auckland, New

Zealand). Possible chimera formation during the sequences was checked using the software DECIPHER (Wright, Yilmaz and Noguera 2012). The sequences obtained were inserted in the BLASTn (Basic Local Alignment and Search Tool for Nucleotides) database and the results were analysed. The sequences associated with this study were deposited in the GenBank database under the accession numbers ON311284 and ON311285.

Phylogenetic Analysis

A total of 58 sequences were used in the final analysis, including 2 strains of *Gloeobacter violaceus* as an outgroup, 56 sequences of cyanobacteria, including type, reference and related strains belonging to the orders Pseudanabaenales and Synechococcales were retrieved from GenBank (National Center for Biotechnology Information, NCBI, Bethesda, MD, USA), and 2 sequences of isolates obtained in this work. Multiple sequence alignment was carried out using ClustalW in MEGA7 (Thompson, Higgins and Gibson 1994; Kumar, Stecher and Tamura 2016), and sequences were manually proofread and edited. The best fit model was assessed using jModelTest 2.1.10 (Darriba *et al.* 2012) according to the Bayesian information criterion (BIC) and Akaike information criterion (AIC) scores. Maximum likelihood (ML) analysis was carried out using substitution model GTR+G+I with 1000 bootstrap resampling replicates using the MEGA7 software (Kumar, Stecher and Tamura 2016). The final phylogenetic tree was visualized and edited on iTOL (Interactive Tree of Life) (Letunic and Bork 2021).

Light Microscopy and Morphological Characterization

Morphological features (e.g., cell dimensions, shape, colour, sheath, constriction at cross walls, specialized cells, or shape of apical cells) of cyanobacterial strains isolated in this work were examined and imaged using a Leica DMLB light microscope coupled to a Leica ICC50

HD digital camera (Leica Microsystems, Germany). For each strain, microphotographs were taken using 400x and 1000x magnifications. Morphometric measurements were then performed using the image analysis software Leica Application Suite version 4.2.0 (Leica Microsystems). Cell dimensions were determined by measuring at least 20-30 cells for each strain along different positions of the slide preparation.

Biofilm Formation Assay

Cyanobacterial isolates were grown in 750 ml of Z8 medium (Kotai 1972) supplemented with 25 $g.l^{-1}$ of synthetic sea salts (Tropic Marin) and B_{12} vitamin (Sigma Aldrich, Merck, Saint Louis, MO, USA), under 14 h light (10–30 µmol photons m^{-2} s^{-1})/10 h dark cycles at 25 °C. To assess the biofilm-forming ability of both strains on different surfaces, biofilms were developed on commercial Perspex (Poly(methyl methacrylate)) surfaces (Neves & Neves, Lda, Portugal) and glass (Vidraria Lousada, Lda, Portugal) coupons (1 cm^2). Surface sterilization and preparation were performed as previously described (Romeu *et al.* 2019). Biofilms were formed on agitated 12-well microtiter plates (VWR International, Carnaxide, Portugal) since this platform was shown to mimic the hydrodynamic conditions found in marine environments (Romeu *et al.* 2019). To attain the shear rate values of aquatic environments, such as those found in a ship hull in a harbor (Bakker *et al.* 2003) and in partially submerged or even moored equipment and devices (average shear rate of 40 s^{-1}), microtiter plates were incubated at 25 °C in an orbital shaker with a 25 mm orbital diameter (Agitorb 200ICP, Norconcessus, Portugal) at 185 rpm (Romeu *et al.* 2019). Biofilm formation in this system was shown to predict the biofouling behavior observed upon immersion in the sea for prolonged periods (Silva *et al.* 2021). Prior to inoculation, the cyanobacterial suspensions were adjusted to a chlorophyll *a* concentration of 1.5 $µg.ml^{-1}$ since chlorophyll *a* is commonly used as a biomass indicator in aquatic environments

(Romeu *et al.* 2019, 2021). Briefly, 2 ml of cyanobacterial suspension were incubated at 4 ºC in the dark for maximal chlorophyll *a* extraction. After 24 h, the samples were centrifuged at 3,202 *g* (Eppendorf Centrifuge 5810R, Hamburg, Germany) for 5 min at room temperature, and the supernatant was transferred to a glass cuvette. The absorbance at 750 nm (turbidity), 665 nm (chlorophyll *a*), and 652 nm (chlorophyll *b*) were determined using a V-1200 spectrophotometer (VWR International China Co., Ltd, Shanghai, China). The chlorophyll *a* concentration was calculated through the following equation (Porra, Thompson and Kriedemann 1989):

$$\text{Chl } a \text{ } (\mu\text{g.ml mg}^{-1}) = 16.29 \times A^{665} - 8.54 \times A^{652} \qquad (1)$$

These measurements were assessed in triplicate, and dilutions were performed using Z8 medium supplemented with 25 $g.l^{-1}$ of synthetic sea salts and vitamin B_{12} (Sigma Aldrich, Merck, Saint Louis, MO, USA). Then, a volume of 3 ml of each cyanobacterial suspension (previously adjusted to chlorophyll *a* concentration of 1.5 $\mu g.ml^{-1}$) was inoculated in each well, in which coupons of each surface were previously fixed with transparent double-sided adhesive tape. Biofilm development was followed for 49 days (seven weeks) since it is accepted that a two-month interval is the minimum duration for economically viable underwater monitoring systems (Blain *et al.* 2004; Romeu *et al.* 2019). During this incubation time, the medium was replaced twice a week. Moreover, to mimic real light exposure periods, a photoperiod of 14 h light (8-10 µmol photons m^{-2} s^{-1})/10 h dark cycles was applied.

Biofilm Analysis

Biofilm analysis was performed every seven days, in which two coupons of each surface were analysed. The culture medium was carefully removed by gentle pipetting, and the wells

were filled with 3 ml of sterile sodium chloride solution (8.5 $g.l^{-1}$) (Romeu *et al.* 2019). The solution was carefully removed to eliminate loosely attached cyanobacteria and subsequently, the wells were filled again with 3 ml of sterile sodium chloride solution to evaluate the thickness and structure of the cyanobacterial biofilms by Optical Coherence Tomography (OCT). To complement the characterization of cyanobacterial biofilms, the determination of their wet weight and chlorophyll *a* content was also performed over the seven weeks. At the last sampling point (49 days), cyanobacterial biofilms of both strains formed on both surfaces were also analysed by Confocal Laser Scanning Microscopy (CLSM).

Optical Coherence Tomography (OCT)

Images from cyanobacterial biofilms developed on both surfaces were captured as reported in Romeu et al. (2019). For each coupon, 2D imaging was performed with a minimum of 3 fields of view to ensure the reliability and accuracy of the results obtained. Image analysis was performed using a routine developed in the Image Processing Toolbox from MATLAB 8.0 and Statistics Toolbox 8.1 (The MathWorks, Inc., Natick, Massachusetts, USA) as described in Romeu et al. (2020). The mean of biofilm thickness was calculated based on the distance between the biofilm bottom and the upper contour line according to the following equation *(2)*:

$$\bar{L}_F = \frac{1}{N}\sum_{i=1}^{N} L_{F,i} \qquad (2)$$

where $L_{F,i}$ is a local biofilm thickness measurement at location *i, N* equals the number of thickness measurements, and $\bar{L}_F$ is the mean biofilm thickness.

Wet Weight Determination and Chlorophyll a Quantification

After OCT analysis, the determination of the biofilm wet weight and chlorophyll *a* content was performed as previously reported (Romeu *et al.* 2021). To determine the wet weight, sterile sodium chloride solution (8.5 $g.l^{-1}$) was carefully removed from the wells, and coupons were detached and weighed. The biofilm wet weight was obtained as the difference from the initial coupon weight, which was determined prior to inoculation. Subsequently, cyanobacterial cells were detached from the coupons by immersing each coupon in 2 ml of 8.5 $g.l^{-1}$ sodium chloride solution and vortexing (Romeu *et al.* 2019). The suspensions were incubated for 24 h at 4 ºC in the dark, and chlorophyll *a* determination was performed through Equation 1.

Confocal Laser Scanning Microscopy (CLSM)

At the last sampling point (day 49), additional coupons were removed from the microplates, washed with saline solution, and the biofilms were stained for 10 min with 6 µM cell-permeant nucleic acid markers: biofilms formed by the cyanobacterial strain isolated from Morocco (*Jaaginema* sp. LEGE 191154) were stained with SYTO®9 (a green fluorescent stain; Thermo Fisher Scientific, Waltham, Massachusetts, USA), whereas biofilms formed by the cyanobacterial strain isolated from Cape Verde (*Leptothoe* sp. LEGE 181153) were marked with SYTO®61 (a red fluorescent stain; Thermo Fisher Scientific, Waltham, Massachusetts, USA). Both stains were chosen to match the colours of cyanobacteria pigments visible by optical microscopy, as well as have minimal interference. Each stained biofilm was mounted on a microscopic slide and image acquisition was performed using a Leica TCS SP5 II Confocal Laser Scanning Microscope (Leica Microsystems, Wetzlar, Germany). All biofilms were scanned using a 40× water objective lens (LEICA HCX PL

APO CS 40.0x/1.10WATER UV) using a protocol previously described (Faria et al., 2021a; Faria et al., 2020a) with some modifications. Given the used stains, *Jaaginema* sp. LEGE 191154 biofilms were observed with a 488-nm argon laser, whereas *Leptothoe* sp. LEGE 181153 biofilms were imaged with a 633-nm helium-neon laser. A minimum of five stacks of horizontal-plane images (512 x 512 pixels, corresponding to 387.5 µm x 387.5 µm) with a *z*-step of 1 µm were acquired per sample.

Three-dimensional (3D) projections of the biofilms were constructed from the CLSM acquisitions using the "Easy 3D" function of the IMARIS 9.1 software (Bitplane, Zurich, Switzerland). Biovolume ($\mu m^3.\mu m^{-2}$) was extracted from confocal image series with the plug-in COMSTAT2 (Heydorn *et al.* 2000) run in ImageJ 1.48v software (National Institutes of Health, Bethesda, Maryland, USA).

Statistical Analysis

A total of four replicates (two biological assays with two technical replicates each) were analysed. Data analysis was performed using the statistical program GraphPad Prism® for Windows, version 6.01 (GraphPad Software, Inc., San Diego, California, USA). The D'Agostino-Pearson and Shapiro-Wilk normality tests were performed to check if the data distribution presented a normal distribution. Differences between biofilm wet weight, chlorophyll *a* quantification, biofilm thickness obtained by OCT, and biovolume obtained by CLSM were evaluated using the unpaired, non-parametric Mann-Whitney test since the variables were not normally distributed. The error bars shown in the graphs correspond to the standard deviation of the mean. Statistically significant differences were considered for p-values < 0.05 (corresponding to a confidence level greater than 95%; and asterisks * and ** denote significance where $p < 0.1$ and $p < 0.05$, respectively).

RESULTS AND DISCUSSION

Phylogenetic Analysis

The phylogenetic analysis of the 16S rRNA gene (Figure 2) showed that the sequence from the cyanobacterium isolated from Cape Verde (*Leptothoe* sp. LEGE 181153) belongs to *Leptothoe* clade, a recent genus described by Konstantinou et al. (2019), a clade with previous *Leptolyngbya* members but not related to the true (sensu stricto) *Leptolyngbya* clade. Sequence from the cyanobacterium isolated from Morocco (*Jaaginema* sp. LEGE 191154) fits in *Jaaginema* clade, which consists of *Jaaginema litorale* LEGE 07176, a strain isolated from a wave-exposed rock on the Portuguese Coast (Ramos *et al.* 2018), *Jaaginema geminatum* SM S13 isolated from a hot spring in Iran (Heidari *et al.* 2018), *Jaaginema* sp. PsrJGgm14, from Psoroneria, a hot spring in Greece, *Jaaginema* sp. PMC 1079.18 and *Jaaginema* sp. PMC 1080.18, isolated from a dense periphytic biofilm covering immersed branch fragment, Guadeloupe (Duperron *et al.* 2019), *Jaaginema* sp. TAU-MAC 1418 (Panou and Gkelis 2022), *Jaaginema* sp. ThrJGgm18 from Thermopyles Thermal Springs in Greece and *Jaaginema* sp. IkpSMP32 isolated from Apolon hot spring, also in Greece. The two cyanobacterial isolates obtained in this work were deposited at the Blue Biotechnology and Ecotoxicology Culture Collection (LEGE-CC) located at CIIMAR, Portugal (Ramos *et al.* 2018), under the names of *Leptothoe* sp. LEGE 181153 (cyanobacterial strain isolated from Cape Verde) and *Jaaginema* sp. LEGE 191154 (cyanobacterial strain isolated from Morocco).

Morphological Description

Leptothoe sp. LEGE 181153 filaments present a single trichome per sheath, unbranched, straight to curved, occasionally wavy, densely, and irregularly entangled. Sheaths are colourless, thin, and slightly distinct. Trichomes are cylindrical, slightly constricted at the

cross walls, and pinkish. Cells are typically barrel-shaped, isodiametric to longer than wide, 2.0 ± 0.3 µm in length and 1.5 ± 0-2 µm in width. Cell content is homogeneous. Apical cells are rounded (Figures 3A and 3C).

Jaaginema sp. LEGE 191154 presents blue-green filaments, unbranched, straight to curved, and entangled in clusters. Without sheaths (sometimes with a fine mucilaginous layer around the trichomes). Trichomes can vary from not constricted to slightly constricted at the cross walls. Cells are cylindrical, longer than wide, 4.6 ± 1.1 µm in length and 2.7 ± 0.3 µm in width. Cell content is homogeneous. Apical cells are narrowed or rounded, without calyptra (Figures 3B and 3D).

Biofilm Development

The biofilm-forming capacity of the *Jaaginema* sp. LEGE 191154 and *Leptothoe* sp. LEGE 181153 strains on two different surfaces (glass and Perspex) was assessed. Results obtained for wet weight, chlorophyll *a* content, and biofilm thickness for both cyanobacterial strains over 49 days are presented in Figure 4. The values regarding the biofilm thickness (Figures 4E, F) are indicated from day 21 since the biofilm thickness was below the OCT range on the first two sampling days. Biofilm development was similar for both cyanobacteria, regardless of the surface material, and the major differences between the strains were observed for the biofilm thickness parameter (Figures 4E, F). This tendency was more evident in biofilm thickness values obtained for glass (Figure 4E) from 35 to 49 days, which corresponds to a maturation stage of biofilm development. Interestingly, previous studies performed with filamentous (Romeu *et al.* 2019, 2020, 2021) and coccoid cyanobacteria (Faria *et al.* 2020b) also showed major differences in biofilm development in their maturation phase. The effects of different conditions may be less noticeable in the initial steps of biofilm formation, while the maturation stage promotes significant variances in biofilm composition and structure.

Also noteworthy is the behaviour of both cyanobacterial biofilms developed on glass (Figures 4A, C, E). While for wet weight and biofilm thickness, the values were similar up to 28 days and increased on *Leptothoe* sp. LEGE 181153 biofilms from 35 to 49 days, for chlorophyll *a* quantification, a different trend between cyanobacterial strains was observed over the 49 days. Indeed, biofilm mass and thickness obtained from 35 to 49 days for *Jaaginema* sp. LEGE 191154 was on average 29% and 54% lower, respectively when compared to the values obtained for *Leptothoe* sp. LEGE 181153 strain on the same period (Figures 4A, E). In turn, chlorophyll *a* quantification obtained from 7 to 28 days for *Leptothoe* sp. LEGE 181153 was on average 77% lower when compared to the values obtained for *Jaaginema* sp. LEGE 191154 (Figure 4B), but from 35 to 49 days chlorophyll *a* amount of *Jaaginema* sp. LEGE 191154 biofilms was on average 58% lower when compared to the values obtained for *Leptothoe* sp. LEGE 181153 (Figure 4B), which supports the results obtained for wet weight and biofilm thickness on the same days (Figures 4A, E). Chlorophyll *a* monitorization has been used to follow cyanobacterial biofilm growth (Romeu *et al.* 2019, 2020, 2021). Considering the similarity of values obtained for wet weight and biofilm thickness up to 28 days, and the opposite trend of chlorophyll *a* quantification on this period, two hypotheses arise. First, *Leptothoe* sp. LEGE 181153 biofilms developed from 7 to 28 days may contain a higher percentage of EPS and/or of void spaces/porous structure filled with water, which can contribute to the higher values of biofilm biomass and thickness, having no impact on chlorophyll *a* level. In turn, cyanobacterial cells in these initial stages of biofilm development may be metabolically less active, contributing to the low chlorophyll *a* amount detected. Additional analysis of empty spaces from 2D cross-sectional OCT images obtained for *Leptothoe* sp. LEGE 181153 biofilms formed on glass (Supplementary Data, Figure 1. Evaluation of biofilm empty spaces) revealed that the percentage of empty spaces in biofilms developed in the initial stage (21 and 28 days) was similar to the values obtained for

the later stages of biofilm development (35 and 42 days), and even lower than those obtained for the last day (49 days). Hence, a porous architecture was not detected in the early biofilm growth stage. Moreover, previous studies on filamentous (Romeu *et al.* 2019, 2020, 2022) and coccoid (Faria *et al.* 2020b) cyanobacterial biofilms also showed that in the initial stages of biofilm development, the chlorophyll *a* amount is lower than those detected in the later stages of biofilm development. Therefore, it is more reasonable that *Leptothoe* sp. LEGE 181153 biofilms developed from 7 to 28 days presented metabolically less active cells and consequently low chlorophyll *a* production.

For both cyanobacterial strains, the biofouling potential on the two surfaces (glass and Perspex) was similar (Supplementary Data, Figure 2. Evaluation of biofilm development on different surfaces). The major difference was observed for biofilm thickness obtained for the *Leptothoe* sp. LEGE 181153 strain at day 42 (Supplementary Data, Figure 2E). On this day, a 69 % decrease in biofilm thickness was achieved on Perspex in comparison with biofilms developed on glass. Although Perspex is relatively more hydrophobic than glass (Romeu *et al.* 2019), previous studies which comprise different genera of cyanobacteria and cyanobacteria isolated from different locations also showed that surface hydrophobicity on its own may not have a significant impact on cyanobacterial biofilm development (Romeu *et al.* 2019, 2020; Faria *et al.* 2020b).

Comparing the behavior of the cyanobacterial strains used in this study with strains isolated from the Portuguese coast (through laboratory experiments performed under the same conditions), it was possible to observe that the present cyanobacterial strains revealed higher biofilm development potential (Romeu *et al.* 2019, 2020, 2021). Indeed, based on the results obtained for wet weight, chlorophyll *a* quantification, and biofilm thickness, among the six filamentous cyanobacterial strains isolated from the Portuguese coast, only two, *Nodosilinea* sp. LEGE 06020 (Romeu *et al.* 2019) and *Nodosilinea* sp. LEGE 06145 (Romeu

et al. 2020), showed enhanced biofilm development ability. While both cyanobacterial strains used in this study presented biofilm wet weight, chlorophyll *a* content, and biofilm thickness values between 5 - 40 mg, 0 - 6 μg.cm^{-2} and up to 150 μm, respectively, over the 49 days, the values achieved by *Nodosilinea* sp. LEGE 06020 (Romeu et al. 2019) and *Nodosilinea* sp. LEGE 06145 (Romeu et al. 2020) were between 5 – 50 mg, 0 – 15 μg.cm^{-2} and up to 600 μm.

Figure 5 shows representative 2D cross-sectional images obtained by OCT at 35 and 49 days. This period corresponds to a maturation phase of biofilm development and the time at which major differences in biofilm thickness between the two cyanobacterial strains were observed (Figures 4E, F). The representative 2D cross-sectional images obtained by OCT confirmed the quantitative results obtained from wet weight, chlorophyll *a* quantification and biofilm thickness over these days (Figure 4). Indeed, thicker biofilms were formed by *Leptothoe* sp. LEGE 181153 and the major difference between both cyanobacterial strains was observed for the last day of the experiment (49 days). Alterations in biofilm structure along this maturation stage can also be noted through a qualitative analysis. For instance, biofilms at 35 days appear to be denser than biofilms developed after 49 days, in which some void spaces are visible (Figure 5). Moreover, this finding is more evident for *Leptothoe* sp. LEGE 181153 biofilms, in which a denser structure can be noted at the biofilm bottom and streamers structures are shown at the biofilm top. An adjustment of biofilm structure may be required over time since, with the gradual biofilm growth, the inner layers of biofilms can have limited access to nutrients, oxygen and light (Teodósio *et al.* 2011; Najmuldeen *et al.* 2019; Gloag *et al.* 2020; Peterson *et al.* 2021). Therefore, this can be a vital adaptation strategy to ensure continuous cyanobacterial biofilm development.

At the end of the experiment, the structural differences between the two cyanobacterial biofilms developed on glass and Perspex were also evaluated using CLSM.

Examples of 3D biofilm images are presented in Figure 6 and biovolume values, which provide an estimate of the biomass in the biofilm ($\mu m^3.\mu m^{-2}$), are shown in Figure 7. Once again, it is possible to observe that denser and thicker biofilms were formed by *Leptothoe* sp. LEGE 181153, regardless of the surface used. Indeed, biovolume obtained for *Jaaginema* sp. LEGE 191154 was on average 71% and 58% lower, respectively, when compared to the values obtained for *Leptothoe* sp. LEGE 181153 strain on glass and Perspex, respectively. These results corroborate the quantitative values obtained from biofilm wet weight, chlorophyll *a* concentration and biofilm thickness (Figure 4), as well as the qualitative 2D images obtained from OCT on day 49 (Figure 5). Moreover, 3D biofilm images obtained from CLSM showed different patterns between cyanobacterial strains but also among the two surfaces. While on biofilms formed by *Jaaginema* sp. LEGE 191154 extended and oriented filaments were detected, tangled and contracted filaments were formed by *Leptothoe* sp. LEGE 181153 (Figure 6). In turn, filaments of biofilms formed on glass appeared individualized and distanced from each other, while on Perspex the filaments have a cohesive architecture (Figure 6). Moreover, biovolume values obtained on glass range from 23 to 80 $\mu m^3.\mu m^{-2}$, and on Perspex from 47 to 112 $\mu m^3.\mu m^{-2}$ (Figure 7). Unlike the porous structure of the biofilms developed on glass, the biofilms of both strains formed on the Perspex seem to have some organic matter such as EPS filling the voids (Figure 7). Previous studies showed that the EPS abundance is more dependent on the environmental conditions (Mota *et al.* 2015) or the intrinsic characteristics of the organisms rather than on the physical and chemical features of the substratum (Del Mondo *et al.* 2018). However, a recent paper revealed that EPS amount can also be related to biofilm production on different surfaces (Maruthanayagam *et al.* 2020). Indeed, Maruthanayagam and his coworkers showed that cyanobacteria produced higher amounts of EPS on hydrophobic polymethyl methacrylate than on the hydrophilic glass surface.

The isolation and characterization of cyanobacterial strains are an important endeavour, due to their potential as new sources of added-value compounds, as well as their adverse and harmful impact on marine biofouling. In this work, two different cyanobacterial strains from under-explored locations in Morocco and Cape Verde were isolated and identified. Both strains showed the capacity to form biofilms, but *Leptothoe* sp. LEGE 181153 proved to be a better biofilm former than *Jaaginema* sp. LEGE 191154 under the hydrodynamic and nutritional conditions tested. Although no significant differences were found in biofilms developed by the same cyanobacterial strain on different surfaces, images obtained by CLSM denoted that biofilms formed on Perspex were denser. Thus, the biofilms of *Leptothoe* sp. LEGE 181153 may be more harmful in marine environments where this surface material is present. Additional assays may evaluate the expression of virulence, adhesion and biofilm development factors by the use of omics approaches to complement the present study (Babele, Kumar and Chaturvedi 2019; Romeu *et al.* 2022). Additionally, to consider the biofilm forming potential of these cyanobacterial strains in real marine environments, it would be interesting to immerse these surfaces in the sea water for prolonged periods, as already performed by the group for other promising coatings against marine biofouling (Silva *et al.* 2021).

FUNDING

This work was financially supported by: LA/P/0045/2020 (ALiCE), UIDB/00511/2020 and UIDP/00511/2020 (LEPABE), funded by national funds through FCT/MCTES (PIDDAC); project HealthyWaters (NORTE-01-0145-FEDER-000069), supported by Norte Portugal Regional Operational Programme (NORTE 2020), under the PORTUGAL 2020 Partnership Agreement, through the European Regional Development Fund (ERDF); project EMERTOX (grant 734748), funded by H2020-MSCA-RISE 2016; Strategic Funding UIDB/04423/2020

and UIDP/04423/2020 through national funds provided by the Foundation for Science and Technology (FCT) and the European Regional Development Fund (ERDF) in the framework of the program PT2020. M.J.R and L.C.G. thank the Portuguese Foundation for Science and Technology (FCT) for the financial support of her PhD grant (SFRH/BD/140080/2018), and a work contract through the Scientific Employment Stimulus—Individual Call—[CEECIND/01700/2017], respectively.

ACKNOWLEDGEMENTS

J.M., R.S. and V.V. would like to thank Prof. Brahim Sabour from Faculty of Sciences El Jadida, University Chouaib Doukkali for all the help sampling in Morocco.

CONFLICT OF INTEREST

The authors declare that they have no conflict of interest.

REFERENCES

Anderson O. Marine and estuarine natural microbial biofilms: ecological and biogeochemical dimensions. *AIMS Microbiol* 2016;**2**:304–31.

Antunes J, Leão P, Vasconcelos V. Marine biofilms: diversity of communities and of chemical cues. *Environ Microbiol Rep* 2019;**11**:287–305.

Antunes JT, Sousa AGG, Azevedo J *et al.* Distinct Temporal Succession of Bacterial Communities in Early Marine Biofilms in a Portuguese Atlantic Port. *Front Microbiol* 2020;**11**:1–17.

Babele PK, Kumar J, Chaturvedi V. Proteomic De-regulation in cyanobacteria in response to abiotic stresses. *Front Microbiol* 2019;**10**:1–22.

Bakker DP, Plaats A Van Der, Verkerke GJ *et al.* Comparison of velocity profiles for

different flow chamber designs used in studies of microbial adhesion to surfaces. *Appl Environ Microbiol* 2003;**69**:6280–7.

Bannister J, Sievers M, Bush F *et al.* Biofouling in marine aquaculture: a review of recent research and developments. *Biofouling* 2019;**35**:631–48.

Berg M, Sutula M. *Factors Affecting the Growth of Cyanobacteria with Special Emphasis on the Sacramento-San Joaquin Delta*., 2015.

Bharti A, Velmourougane K, Prasanna R. Phototrophic biofilms: diversity, ecology and applications. *J Appl Phycol* 2017;**29**:2729–44.

Blain S, Guillou J, Tréguer PJ *et al.* High frequency monitoring of the coastal marine environment using the MAREL buoy. *J Environ Monit* 2004;**6**:569–75.

Bragg JG, Thomas D, Baudouin-Cornu P. Variation among species in proteomic sulphur content is related to environmental conditions. *Proceedings Biol Sci* 2006;**273**:1293–300.

Breinlinger S, Phillips TJ, Haram BN *et al.* Hunting the eagle killer: A cyanobacterial neurotoxin causes vacuolar myelinopathy. *Science (80-)* 2021;**371**, DOI: 10.1126/science.aax9050.

Cai W, Arias CR. Biofilm Formation on Aquaculture Substrates by Selected Bacterial Fish Pathogens. *J Aquat Anim Heal* 2017;**29**:95–104.

Caruso G. Microbial colonization in marine environments: Overview of current knowledge and emerging research topics. *J Mar Sci Eng* 2020;**8**:1–22.

Carvalho CCCR. Marine biofilms: A successful microbial strategy with economic implications. *Front Mar Sci* 2018;**5**:1–11.

Claessen D, Rozen DE, Kuipers OP *et al.* Bacterial solutions to multicellularity: a tale of biofilms, filaments and fruiting bodies. *Nat Rev Microbiol* 2014;**12**:115–24.

Coleman ML, Chisholm SW. Code and context: Prochlorococcus as a model for cross-scale

biology. *Trends Microbiol* 2007;**15**:398–407.

Croft MT, Warren MJ, Smith AG. Algae need their vitamins. *Eukaryot Cell* 2006;**5**:1175–83.

Dang H, Lovell CR. Microbial Surface Colonization and Biofilm Development in Marine Environments. *Microbiol Mol Biol Rev* 2016;**80**:91–138.

Darriba D, Taboada GL, Doallo R *et al.* jModelTest 2: more models, new heuristics and parallel computing. *Nat Methods* 2012;**9**:772.

Davidson IC, Brown CW, Sytsma MD *et al.* The role of containerships as transfer mechanisms of marine biofouling species. *Biofouling J Bioadhesion Biofilm Res* 2009;**25**:645–55.

Davies P, Rajapakse YDS. *Durability of Composites in a Marine Environment*. Springer Netherlands, 2013.

Delauney L, Compare C, Lehaitre M. Biofouling protection for marine environmental sensors. *Ocean Sci* 2010;**6**:503–11.

Dobretsov S, Rittschof D. Love at first taste: Induction of larval settlement by marine microbes. *Int J Mol Sci* 2020;**21**, DOI: 10.3390/ijms21030731.

Duperron S, Beniddir MA, Durand S *et al.* New Benthic Cyanobacteria from Guadeloupe Mangroves as Producers of Antimicrobials. *Mar Drugs* 2019;**18**, DOI: 10.3390/md18010016.

Faria S, Gomes LC, Teixeira-Santos R *et al.* Developing new marine antifouling surfaces: Learning from single-strain laboratory tests. *Coatings* 2021a;**11**:1–11.

Faria S, Teixeira-Santos R, Morais J *et al.* The association between initial adhesion and cyanobacterial biofilm development. *FEMS Microbiol Ecol* 2021b;**97**:fiab052.

Faria S, Teixeira-Santos R, Romeu MJ *et al.* Unveiling the antifouling performance of different marine surfaces and their effect on the development and structure of cyanobacterial biofilms. *Microorganisms* 2021c;**9**:1102.

Faria SI, Teixeira-Santos R, Gomes LC *et al.* Experimental assessment of the performance of two marine coatings to curb biofilm formation of microfoulers. *Coatings* 2020a;**10**, DOI: 10.3390/COATINGS10090893.

Faria SI, Teixeira-Santos R, Romeu MJ *et al.* The Relative Importance of Shear Forces and Surface Hydrophobicity on Biofilm Formation by Coccoid Cyanobacteria. *Polymers (Basel)* 2020b;**12**:653.

Foster JS, Green SJ, Ahrendt SR *et al.* Molecular and morphological characterization of cyanobacterial diversity in the stromatolites of highborne cay, bahamas. *ISME J* 2009;**3**:573–87.

Georgiades E, Scianni C, Davidson I *et al.* The Role of Vessel Biofouling in the Translocation of Marine Pathogens: Management Considerations and Challenges. *Front Mar Sci* 2021;**8**:1–20.

Gloag ES, Fabbri S, Wozniak DJ *et al.* Biofilm mechanics: Implications in infection and survival. *Biofilm* 2020;**2**:100017.

Heidari F, Zima J, Riahi H *et al.* New simple trichal cyanobacterial taxa isolated from radioactive thermal springs. *Fottea* 2018;**18**:137–49.

Helliwell KE, Lawrence AD, Holzer A *et al.* Cyanobacteria and Eukaryotic Algae Use Different Chemical Variants of Vitamin B12. *Curr Biol* 2016;**26**:999–1008.

Heydorn A, Nielsen AT, Hentzer M *et al.* Quantification of biofilm structures by the novel computer program COMSTAT. *Microbiology* 2000;**146**:2395–407.

Huisman J, Codd GA, Paerl HW *et al.* Cyanobacterial blooms. *Nat Rev Microbiol* 2018;**16**:471–83.

Hunsucker KZ, Vora GJ, Hunsucker JT *et al.* Biofilm community structure and the associated drag penalties of a groomed fouling release ship hull coating. *Biofouling* 2018;**34**:162–72.

King RK, Flick GJ, Smith SA *et al.* Comparison of bacterial presence in biofilms on different materials commonly found in recirculating aquaculture systems. *J Appl Aquac* 2006;**18**:79–88.

Konstantinou D, Gerovasileiou V, Voultsiadou E *et al.* Sponges-cyanobacteria associations: Global diversity overview and new data from the Eastern Mediterranean. *PLoS One* 2018;**13**:1–22.

Konstantinou D, Voultsiadou E, Panteris E *et al.* Leptothoe, a new genus of marine cyanobacteria (Synechococcales) and three new species associated with sponges from the Aegean Sea. *J Phycol* 2019;**55**:882–97.

Kotai J. Instructions for the Preparation of Modified Nutrient Solution Z8 for Algae. 1972:5.

Ku C, Nelson-Sathi S, Roettger M *et al.* Endosymbiotic origin and differential loss of eukaryotic genes. *Nature* 2015;**524**:427–32.

Kumar S, Stecher G, Tamura K. MEGA7: Molecular Evolutionary Genetics Analysis version 7.0 for bigger datasets. *Mol Biol Evol* 2016:msw054.

Lau NS, Matsui M, Abdullah AAA. Cyanobacteria: Photoautotrophic Microbial Factories for the Sustainable Synthesis of Industrial Products. *Biomed Res Int* 2015;**2015**, DOI: 10.1155/2015/754934.

Letunic I, Bork P. Interactive Tree Of Life (iTOL) v5: an online tool for phylogenetic tree display and annotation. *Nucleic Acids Res* 2021;**49**:W293–6.

Limoli DH, Jones CJ, Wozniak DJ. Bacterial Extracellular Polysaccharides in Biofilm Formation and Function. *Microbiol Spectr* 2015;**3**, DOI: 10.1128/microbiolspec.MB-0011-2014.

Lv J, Li N, Niu DK. Association between the availability of environmental resources and the atomic composition of organismal proteomes: Evidence from Prochlorococcus strains living at different depths. *Biochem Biophys Res Commun* 2008;**375**:241–6.

Lyons TW, Reinhard CT, Planavsky NJ. The rise of oxygen in Earth's early ocean and atmosphere. *Nature* 2014;**506**:307–15.

Manirafasha E, Ndikubwimana T, Zeng X *et al.* Phycobiliprotein: Potential microalgae derived pharmaceutical and biological reagent. *Biochem Eng J* 2016;**109**:282–96.

Mansour A, Liu D. *The Principles of Naval Architecture Series: Strength of Ships and Ocean Structures*. Paulling JR (ed.). Jersey City, NJ: The Society of Naval Architects and Marine Engineers, 2008.

Martiny AC, Coleman ML, Chisholm SW. Phosphate acquisition genes in Prochlorococcus ecotypes: Evidence for genome-wide adaptation. *Proc Natl Acad Sci U S A* 2006;**103**:12552–7.

Maruthanayagam V, Basu S, Bhattacharya D *et al.* Effects of surface material on growth pattern and bioactive exopolymers production of intertidal cyanobacteria Phormidium sp. *Indian J Geo-Marine Sci* 2020;**49**:1669–77.

Molland AF. Ship design, construction and operation. *The Maritime Engineering Reference Book: A Guide to Ship Design, Construction and Operation*. Butterworth-Heinemann, 2008.

Del Mondo A, Pinto G, Carbone DA *et al.* Biofilm architecture on different substrates of an Oculatella subterranea (Cyanobacteria) strain isolated from Pompeii archaeological site (Italy). *Environ Sci Pollut Res* 2018;**25**:26079–89.

Moore LR, Ostrowski M, Scanlan DJ *et al.* Ecotypic variation in phosphorus-acquisition mechanisms within marine picocyanobacteria. *Aquat Microb Ecol* 2005;**39**:257–69.

Van Mooy BAS, Rocap G, Fredricks HF *et al.* Sulfolipids dramatically decrease phosphorus demand by picocyanobacteria in oligotrophic marine environments. *Proc Natl Acad Sci U S A* 2006;**103**:8607–12.

Mota R, Pereira SB, Meazzini M *et al.* Effects of heavy metals on Cyanothece sp. CCY 0110

growth, extracellular polymeric substances (EPS) production, ultrastructure and protein profiles. *J Proteomics* 2015;**120**:75–94.

Mullineaux CW. Co-existence of photosynthetic and respiratory activities in cyanobacterial thylakoid membranes. *Biochim Biophys Acta* 2014;**1837**:503–11.

Najmuldeen H, Alghamdi R, Alghofaili F *et al.* Functional assessment of microbial superoxide dismutase isozymes suggests a differential role for each isozyme. *Free Radic Biol Med* 2019;**134**:215–28.

Pagels F, Guedes AC, Amaro HM *et al.* Phycobiliproteins from cyanobacteria: Chemistry and biotechnological applications. *Biotechnol Adv* 2019;**37**:422–43.

Panou M, Gkelis S. Unravelling unknown cyanobacteria diversity linked with HCN production. *Mol Phylogenet Evol* 2022;**166**:107322.

Papadatou M, Robson SC, Dobretsov S *et al.* Marine biofilms on different fouling control coating types reveal differences in microbial community composition and abundance. *Microbiologyopen* 2021;**10**:1–17.

Peterson BW, van der Mei HC, Sjollema J *et al.* A Distinguishable Role of eDNA in the Viscoelastic Relaxation of Biofilms. *MBio* 2021;**4**:e00497-13.

Pointing SB, Belnap J. Microbial colonization and controls in dryland systems. *Nat Rev Microbiol* 2012;**10**:551–62.

Porra R, Thompson W, Kriedemann P. Determination of accurate extinction coefficients and simultaneous equations for assaying chlorophylls a and b extracted with four different solvents: verification of the concentration of chlorophyll standards by atomic absorption spectroscopy. *Biochim Biophys Acta* 1989;**975**:384–94.

Ramos V, Morais J, Castelo-Branco R *et al.* Cyanobacterial diversity held in microbial biological resource centers as a biotechnological asset: the case study of the newly established LEGE culture collection. *J Appl Phycol* 2018;**30**:1437–51.

Rippka R. Isolation and purification of cyanobacteria. *Methods Enzymol* 1988;**167**:3–27.

Romeu MJ, Alves P, Morais J *et al.* Biofilm formation behaviour of marine filamentous cyanobacterial strains in controlled hydrodynamic conditions. *Environ Microbiol* 2019;**21**:4411–24.

Romeu MJ, Domínguez-pérez D, Almeida D *et al.* Hydrodynamic conditions affect the proteomic profile of marine biofilms formed by filamentous cyanobacterium. *npj Biofilms Microbiomes* 2022;**8**:80.

Romeu MJ, Domínguez-Pérez D, Almeida D *et al.* Characterization of planktonic and biofilm cells from two filamentous cyanobacteria using a shotgun proteomic approach. *Biofouling* 2020;**36**:631–45.

Romeu MJ, Domínguez-Pérez D, Almeida D *et al.* Quantitative proteomic analysis of marine biofilms formed by filamentous cyanobacterium. *Environ Res* 2021:111566.

Rossi F, De Philippis R. Role of cyanobacterial exopolysaccharides in phototrophic biofilms and in complex microbial mats. *Life* 2015;**5**:1218–38.

Roy GJ. *Notes on Instrumentation and Control (Marine Engineering)*. Oxford, Boston: Newnes, 1994.

Rusch DB, Halpern AL, Sutton G *et al.* The Sorcerer II Global Ocean Sampling expedition: Northwest Atlantic through eastern tropical Pacific. *PLoS Biol* 2007;**5**:0398–431.

Schirrmeister BE, Antonelli A, Bagheri HC. The origin of multicellularity in cyanobacteria. *BMC Evol Biol* 2011;**11**:45.

Silva ER, Tulcidas A V, Ferreira O *et al.* Assessment of the environmental compatibility and antifouling performance of an innovative biocidal and foul-release multifunctional marine coating. *Environ Res* 2021;**198**:111219.

Singh R, Parihar P, Singh M *et al.* Uncovering potential applications of cyanobacteria and algal metabolites in biology, agriculture and medicine: Current status and future

prospects. *Front Microbiol* 2017;**8**:1–37.

Taylor DA. *Introduction to Marine Engineering*. Butterworth-Heinemann, 1996.

Teodósio JS, Simões M, Melo LF *et al.* Flow cell hydrodynamics and their effects on E. coli biofilm formation under different nutrient conditions and turbulent flow. *Biofouling* 2011;**27**:1–11.

Thompson JD, Higgins DG, Gibson TJ. CLUSTAL W: improving the sensitivity of progressive multiple sequence alignment through sequence weighting, position-specific gap penalties and weight matrix choice. *Nucleic Acids Res* 1994;**22**:4673–80.

Vermaas WFJ. *Photosynthesis and Respiration in Cyanobacteria*., 2001.

Vincent WF. Cyanobacterial Dominance in the Polar Regions. In: Whitton BA, Potts M (eds.). *The Ecology of Cyanobacteria*. Dordrecht: Springer Netherlands, 2000, 321–40.

Wright ES, Yilmaz LS, Noguera DR. DECIPHER, a search-based approach to chimera identification for 16S rRNA sequences. *Appl Environ Microbiol* 2012;**78**:717–25.

Figure 1. Sampling locations: A) dried soil crust near Mrizika Beach, Morocco; B) green mat on ramp port for boats at Calhau, São Vicente Island, Cape Verde.

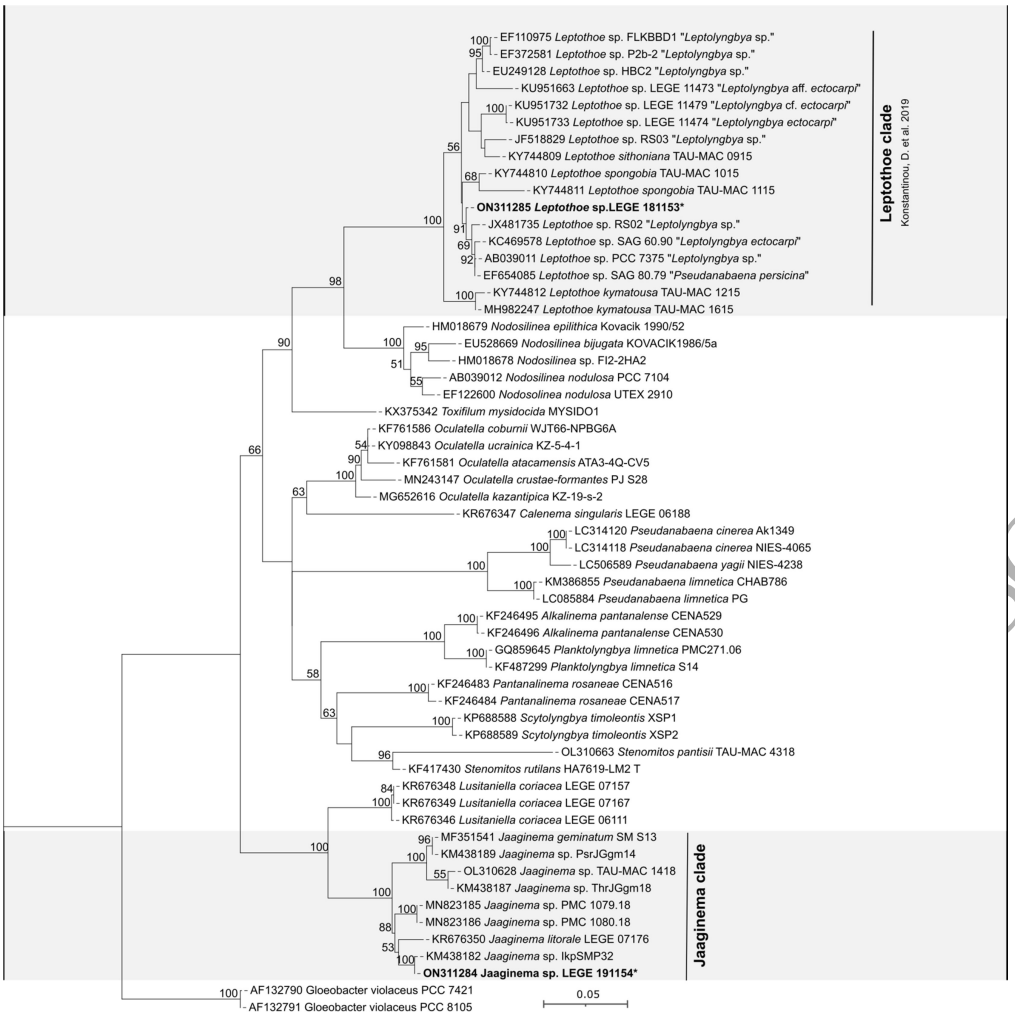

Figure 2. Maximum likelihood (ML) phylogenetic tree based on 58 partial 16S rRNA gene sequences of cyanobacterial strains belonging to the orders Pseudanabaenales and Synechococcales. *Gloeobacter violaceus* PCC 7421 and *Gloeobacter violaceus* PCC 8105 were used as outgroups. Phylogenetic positions of *Leptothoe* sp. LEGE 181153 and *Jaaginema* sp. LEGE 191154 are indicated in bold and with a black star. Bootstrap values over 50% are indicated at the nodes. Strains labelled with quotes indicate that names correspond to Genbank labels.

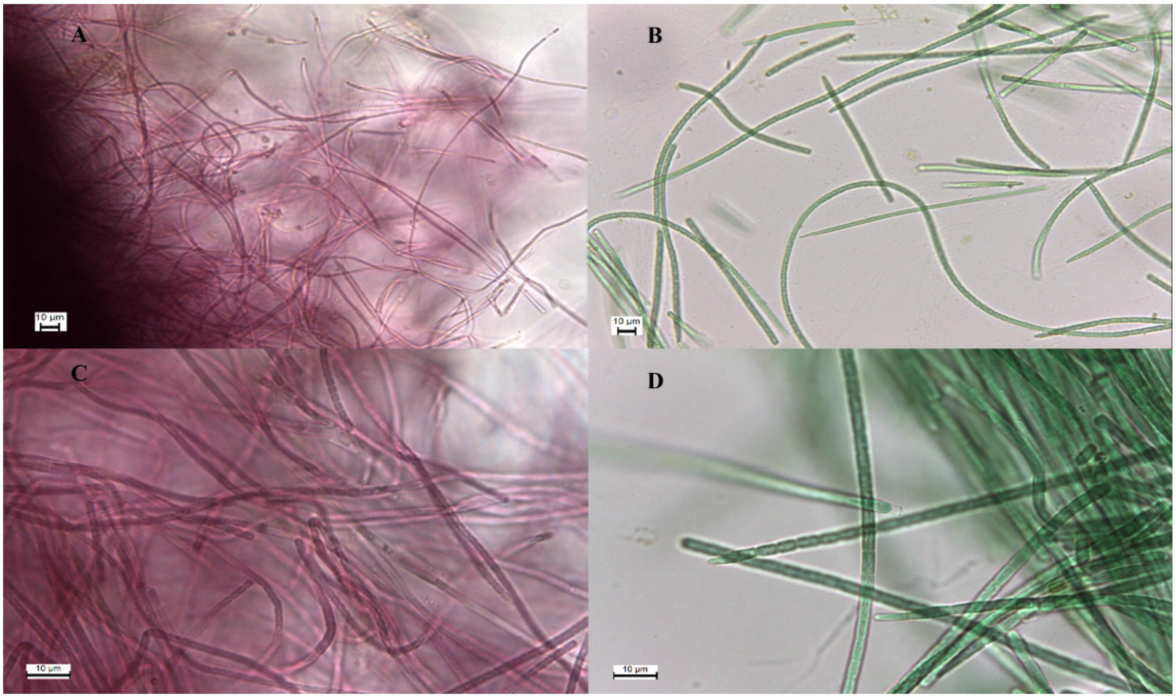

Figure 3. Light microscopy of A) *Leptothoe* sp. LEGE 181153 (400x); B) *Jaaginema* sp. LEGE 191154 (400x); C) *Leptothoe* sp. LEGE 181153 (1000x); D) *Jaaginema* sp. LEGE 191154 (1000x). Scale bars = 10 µm.

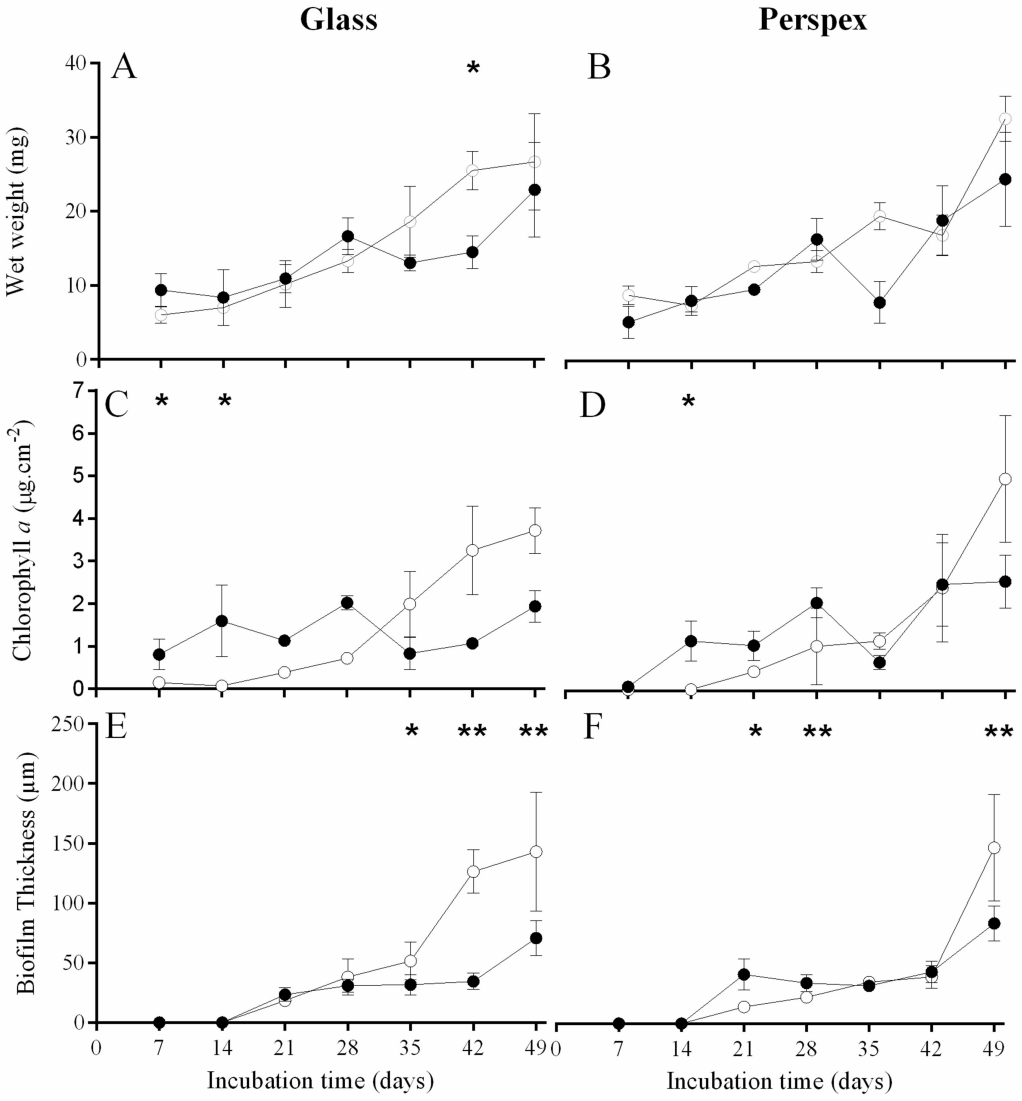

Figure 4. Evaluation of cyanobacterial biofilm development. The parameters analysed refer to wet weight (A, B), chlorophyll *a* (C, D), and biofilm thickness (E, F). Biofilms of *Jaaginema* sp. LEGE 191154 (closed circles) and *Leptothoe* sp. LEGE 181153 (open circles) were formed on glass or perspex at an average shear rate of 40 s^{-1} for 49 days. Symbols * and ** indicate statistically different values for $p < 0.1$ and $p < 0.05$ on each incubation time, respectively.

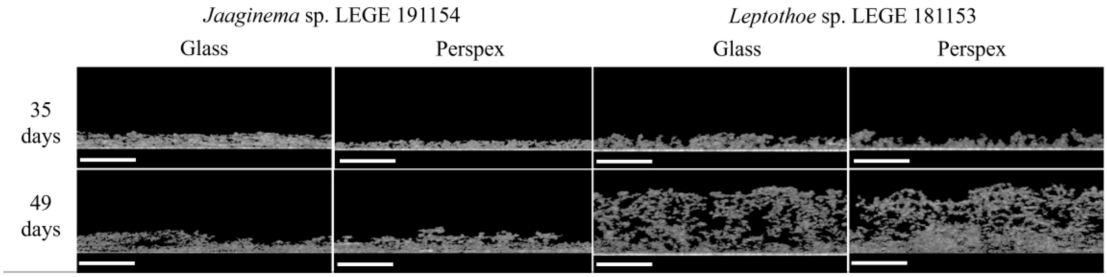

Figure 5. 2D cross-sectional OCT images of cyanobacterial biofilms formed at 35 and 49 days on glass and perspex. Scale bar = 200 µm.

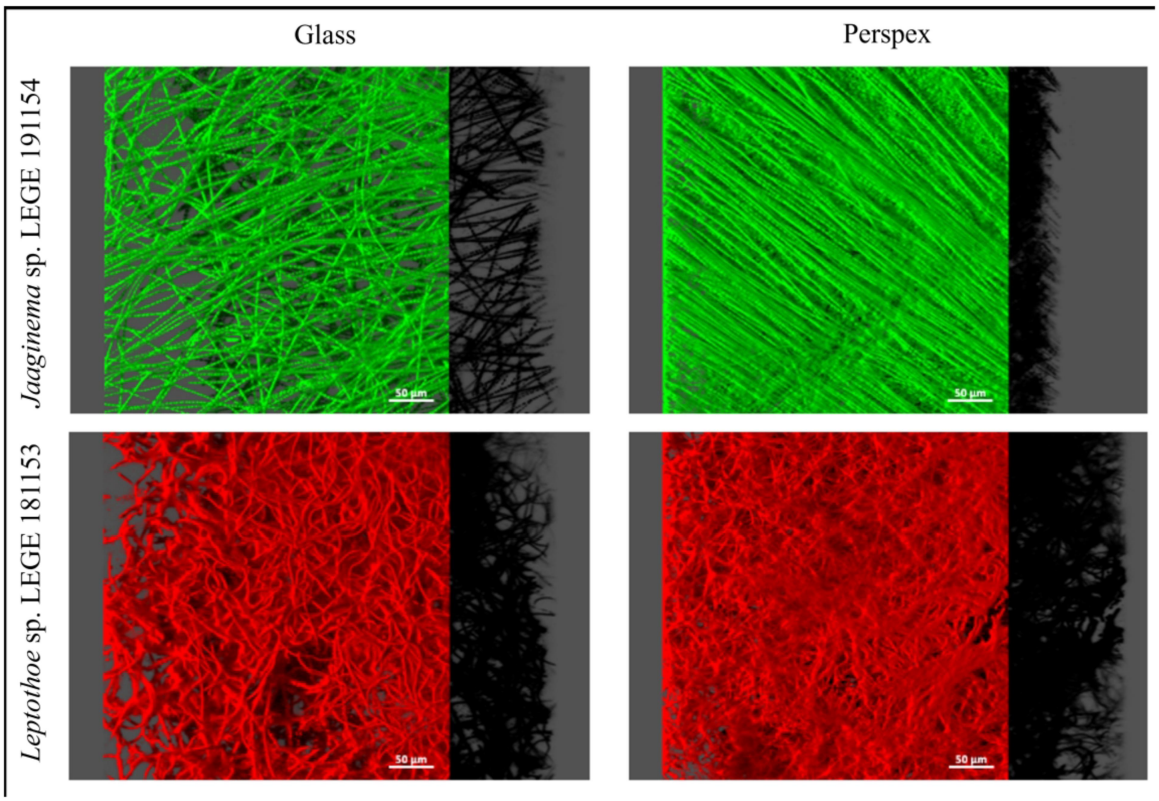

Figure 6. CLSM images of cyanobacterial biofilms formed after 49 days on glass and perspex. Scale bar = 50 µm.

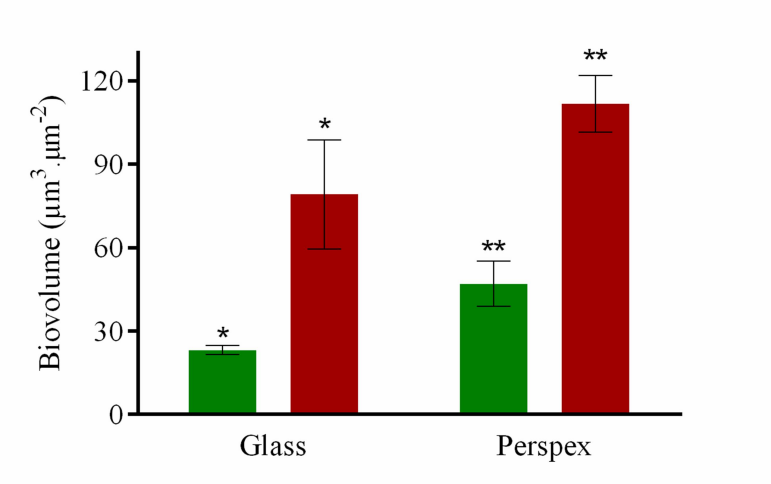

Figure 7. Biovolume obtained from CLSM *z*-stacks of *Jaaginema* sp. LEGE 191154 (green bars) and *Leptothoe* sp. LEGE 181153 (red bars) biofilms formed after 49 days on glass and perspex. Symbols * and ** indicate statistically different values for $p < 0.1$ and $p < 0.05$ between both cyanobacterial strains on the same surface, respectively.

Table 1. Oligonucleotide primers used for 16s rRNA amplification.

Primer	Sequence 5'-3'	Reference
27F	AGAGTTTGATCCTGGCTCAG	(Lane, 1991)
359F	GGGGAATYTTCCGCAATGGG	(Nübel et al., 1997)
781R	GACTACWGGGGTATCTAATCCCWTT	(Nübel et al., 1997)
1494R	TACGGCTACCTTGTTACGAC	(Lane, 1991)
23S30R	CTTCGCCTCTGTGTGCCTAGGT	(Lepère et al., 2000)